Biochimica et Biophysica Acta, 1101 (1992) 121–124

BBABIO 40261

Rapid Report

Near-infrared Yb^{3+} vibronic sideband spectroscopy: application to Ca^{2+}-binding proteins

Tony A. Mattioli [a], Cécile Roselli [b] and Alain Boussac [b]

[a] *Service de Biophysique des Protéines Membranaires and* [b] *Service de Bioénergétique, Département de Biologie Cellulaire et Moléculaire, C.E. Saclay, Gif-sur-Yvette (France)*

(Received 6 April 1992)

Key words: Calcium binding protein; Near-infrared vibronic sideband spectroscopy; Vibrational spectroscopy; Ytterbium; Parvalbumin; Tryptophan fluorescence

We have used near-infrared (NIR) vibronic fluorescence spectroscopy to study the vibrational structure of ligands associated with model complexes of the lanthanide Yb^{3+}. This technique exploits the similar binding properties of the lanthanide Yb^{3+} to probe Ca^{2+}-binding sites in proteins. The (NIR) fluorescence of complexed Yb^{3+} exhibits, in addition to main 0–0 ($^2F_{5/2} \rightarrow {}^2F_{7/2}$) electronic transition of Yb^{3+}, weak vibronic sidebands which provide infrared-like, local vibrational spectra of the chelates (inner sphere ligands) of Yb^{3+}. A similar approach has been used for the lanthanide Gd^{3+} (MacGregor, R.B., Jr. (1989) Arch. Biochem. Biophys. 274, 312–316) which fluoresces in the UV and which is usually complicated by amino-acid residues fluorescing in the same spectral region. In this same spectral region, other complications in studying photosynthetic membranes occur in the form of the excitation wavelength being actinic, promoting photodegradation of the membranes, as well as the reabsorption of Gd^{3+} fluorescence. NIR excitation and fluorescence detection of Yb^{3+} avoid these problems when studying photosynthetic membranes. A preliminary study has been conducted here on rat muscle parvalbumin.

Calcium-binding proteins are currently the subject of much interest. Functional and local conformational properties of many proteins [1–3], including the oxygen-evolving enzyme of higher plants, are modulated by the site-specific binding of Ca^{2+} [4–6].

Ca^{2+} does not lend itself to be directly probed by traditional spectroscopic methods (e.g., optical and EPR). However, EPR spectroscopy in conjunction with Ca^{2+}/Mn^{2+} [7] or Ca^{2+}/Ln^{2+} [8,9] exchange, has been used to probe the nature and distances of atoms interacting with Ca^{2+} in proteins. Trivalent lanthanides have been used to probe Ca^{2+} sites because they are fluorescent and also exhibit Ca^{2+}-like binding properties based largely on the similar size of lanthanides and Ca^{2+} [1,2,9–11]. Most of the fluorescence work has involved measuring the quenching of the lanthanide fluorescence which provides estimates of distances, but not directly the nature, of the ligands binding to the Ca^{2+}/Ln^{3+} ions. However, Gd^{3+} vibronic sideband spectroscopy in the UV has been shown by MacGregor to be effective in model complexes to provide the partial vibrational spectrum of chelates of Gd^{3+} [12] but requires sophisticated time-resolved techniques to eliminate tryptophan fluorescence in real biological samples [13]. We have extended this technique to the near-infrared (NIR) spectral region. Working in the NIR circumvents the tryptophan fluorescence problem because excitation in this spectral region does not induce fluorescence of this amino acid in proteins.

The vibronic sidebands observed in the fluorescence spectrum of the Ln^{3+} complexes are shifted to longer wavelengths with respect to the main $4f$–$4f$ electronic transition of the lanthanide and arise from the dipole–dipole coupling of the electronic transition and the infrared-active vibrational oscillators of the chelates; the shifts in energy (in cm^{-1}) correspond to the vibrational frequency of the chelate oscillators. The vibrations of the chelate chemical groups associated with the ligation of Ln^{3+} are expected to be more active than those modes of chemical groups further from the metal.

The choice of Ln^{3+} ion is important in this application because one needs a single well-isolated electronic transition so that there are no complications and over-

Abbreviations: NIR, near-infrared; VSB, vibronic sideband; RMPA, rat muscle parvalbumin; bipy, 2,2′-bipyridine; DPA, dipicolinic acid; NTA, nitriloacetic acid; Mes, 2-(*N*-morpholino)ethanesulfonic acid.

Correspondence to: T.A. Mattioli, Service de Biophysique des Protéines Membranaires, Départment de Biologie Cellulaire et Moléculaire, C.E. Saclay, 91191 Gif-sur-Yvette Cedex, France.

lap of 0–0 electronic transitions and the respective vibronic sidebands. Yb^{3+} meets this criterion because it has an isolated electronic transition/energy level at about 10000 cm^{-1} and whose absorption band is at about 980 nm [14].

This means that one can excite the fluorescence of Yb^{3+} in a Ca^{2+}-binding protein using laser radiation ranging from about 900 to 990 nm. This has the added benefit that there are no re-absorption problems that occur when exciting Gd^{3+} fluorescence (300–350 nm) in a protein (276–300 nm excitation). More importantly, if the Ca^{2+}-binding protein contains chromophores, as in the case of photosynthetic membranes, these NIR excitation wavelengths will not be actinic or promote photodegradation, as can occur with UV excitation. Also, the fluorescence will not be re-absorbed by the chromophores or protein (only weakly by water). Lastly, if one has a sensitive NIR spectrometer, one can detect the weak vibronic sidebands even at room temperature.

We have tested the feasibility of this NIR vibronic sideband spectroscopic technique with model compounds of Yb^{3+} as well as with rabbit muscle parvalbumin (RMPA), a well-characterized Ca^{2+}-binding protein, with Ca^{2+} exchanged for Yb^{3+} [15]. The VSB spectrum of Yb^{3+} in RMPA compares well with the Gd^{3+} VSB of the same protein [13].

All chemicals were reagent grade or better and were used without further purification. $YbCl_3 \cdot 6H_2O$ and 2,2′-bipyridine were purchased from Aldrich (France), 1-methylimidazole and rat muscle parvalbumin (RMPA) from Sigma. Near-infrared red excitation at 910 nm was provided by a cw Ti:sapphire laser (Spectra Physics Model 3900 S) pumped with an Ar^+ laser (Coherent Innova 100) operating in the all-lines mode at about 8 W. Typically, 200–300 mW was used for NIR excitation. NIR fluorescence spectra were recorded using a Bruker IFS 66 FTIR spectrometer modified for the NIR spectral region and equipped with a Bruker FRA 106 FT Raman module; the spectrometer has been described elsewhere [16]. The liquid samples were contained in a 1 cm quartz cuvette and fluorescence was measured in a 90° geometry. Stray light from the exciting laser was reduced using long-wave pass filters (Corion, LL-1000 and LL-950) positioned in the Jacquinot stop. All spectra were measured at room temperature. Instrumental spectral resolution was 4 cm^{-1}.

All the known Ca^{2+} ligands in proteins are oxygen atoms from the protein backbone or the amino-acid side-chains [2]. Nevertheless, exceptions may occur, as is proposed in Photosystem II (Ref. 4 for a review). Possible artificial Ca^{2+} ligands may be those which possess (i) OH, (ii) COO^-, and (iii) nitrogen-containing groups in the amino-acid side-chains. Thus, as Yb^{3+} chelators we chose (i) water and methanol, (ii) DPA, which is a well-known chelator of Ln^{3+} ions [18], and NTA, which is a specific chelator for trivalent ions, (iii) 1-methylimidazole and 2,2′-bipyridine (bipy).

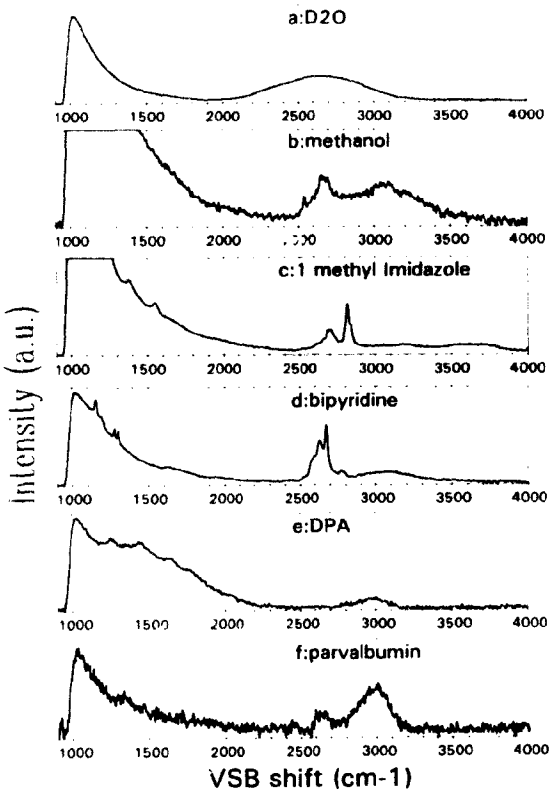

Fig. 1. VSB fluorescence spectra of Yb^{3+} in various ligand coordination environments. The data are plotted in terms of frequency shift (in cm^{-1}) from the 0–0 transition as described in the text. All spectra are at room temperature; laser excitation was 910 nm; laser power was 200–300 mW; spectral resolution was 4 cm^{-1}. (a) 100 mM Yb^{3+} in D_2O; 4000 scans. (b) 500 mM Yb^{3+} in methanol; 2000 scans. (c) 100 mM Yb^{3+} in 1-methylimidazole; 9000 scans. (d) 100 mM Yb^{3+} + 400 mM bipy in ethanol; 12000 scans. (e) 50 mM Yb^{3+} + 250 mM DPA in H_2O; 12000 scans. (f) 5 mM Yb^{3+} + 1 mM RMPA + 0.3 mM sucrose + 10 mM NaCl + 25 mM Mes (pH 6.5) in H_2O; 15000 scans.

Fig. 1a shows the vibronic fluorescence spectrum of 0.1 M Yb^{3+} dissolved in D_2O which exhibits a large vibronic sideband (VSB) at about 2650 cm^{-1} shifted from the intense the $4f$–$4f$ electronic transition of Yb^{3+}. The intense 0–0 fluorescence transition band was observed to be distorted due to the limit of the spectral response of the detector in the FT Raman instrument, and also distorted due to the built-in rejection filter at 1064 nm. The VSB shifts were therefore calculated from the 0–0 level estimated from the measured absorption spectrum maximum of the complex

(974 nm or 10 270 cm^{-1}, which corresponds to a single electronic energy level [17]). This vibronic sideband in Fig. 1a is identified as the OD stretching mode of the D_2O molecules complexed with Yb^{3+}. This shift is that expected from the infrared absorption spectrum of D_2O and also agrees with the vibronic sideband shifts observed using Gd^{3+} complexes [12]. The weaker sideband expected at about 1200–1300 cm^{-1} for this complex corresponding to the bending mode of D_2O is not observed in our spectra due to their relative weakness and interference from the main electronic transition. The observed sideband cannot arise from a Raman effect using 910 nm excitation (as was verified by recording the Raman spectra of D_2O with 910 nm excitation in the absence of Yb^{3+}) because of the excessively large Raman shift this would imply. The fluorescence spectrum of Yb^{3+} complexed with methanol shown in Fig. 1b exhibits a complex set of vibronic sidebands at about 3000 cm^{-1} shift in the OH (about 3100 cm^{-1}) and CH (about 2700 cm^{-1} in Fig. 1b) stretching region of the vibrational spectrum. The shapes and frequency shifts of these resolved vibronic sidebands agree gratifyingly well with the infrared absorption spectrum of methanol and illustrates the high resolution of the apparatus used in this work.

For Yb^{3+} complexes with chelates containing carboxylate groups, one expects to observe sibeband shifts at about 1600 cm^{-1} and about 1400 cm^{-1} based on infrared absorption data of CO_2^- groups. These shifts are clearly seen in the fluorescence spectrum of the Yb^{3+}-DPA complex in Fig. 1e as well as in the spectrum of the Yb^{3+}-NTA complex (data not shown). The enhancement of these CO_2^- modes indicates that these chemical groups are involved in the chelation of Yb^{3+} as expected. The CH modes expected in our VSB spectra at shifts of about 2700–3000 cm^{-1} are very weak in the fluorescence spectrum; this is to be expected, since it is the CO_2^- groups which are involved in the chelation and the CH groups are relatively far removed from the Yb^{3+} ion and thus much weaker in intensity.

The fluorescence spectra for the Yb^{3+} complexes involving the nitrogen-containing ligands 1-methylimidazole and bipy are shown in Figs. 1c and 1d, respectively. These spectra are relatively more intense than the others and highly resolved bands are observed for these complexes are seen in the 2600–2900 cm^{-1} region. There is a complex cluster of bands at about 2700 cm^{-1}, in the same region as the band observed in the Yb^{3+}-methanol complex, which most likely correspond to the -C–H stretches. These frequencies are about 200 cm^{-1} lower than those of the free ligand. In the Yb^{3+}-1-methylimidazole spectrum, however, there is a complex band at about 2830 cm^{-1} which could arise from the higher frequency N–H stretching modes. The observed vibronic sideband shifts agree very well with frequencies observed in the IR spectrum of 1-methylimidazole. The bands at about 1530 and 1330 cm^{-1} (and 1050 cm^{-1}, band not shown in the scale of Fig. 1c) in the Yb^{3+}-1-methylimidazole VSB spectrum match very well with the intense 1520 and 1285 cm^{-1} (and 1082 cm^{-1}) bands observed in the IR absorption spectrum for the free ligand (data not shown). Comparison of Figs. 1c and 1d illustrates that the VSB spectrum of 1-methylimidazole is distinct and can be used as a spectral signature to distinguish it from other nitrogen-containing ligands.

Fig. 1f shows the fluorescence spectrum of 1 mM RMPA and 5 mM Yb^{3+}. Under these conditions we expect that all of the Ca^{2+} in the protein has been exchanged with Yb^{3+} and that the majority of the Yb^{3+} is complexed with H_2O or unspecifically 'attached' to the protein surface. The spectrum is weak and of modest signal-to-noise ratio; however, some features are discernible. The appearance and shape of the vibronic sideband shifted about 3000 cm^{-1} indicates that H_2O is chelating some fraction of the total Yb^{3+} ions, most likely from those in solution. There is also the appearance of a very weak, broad unresolved VSB at about 1500 cm^{-1} which is not resolved but corresponds well with the resolved VSB bands at 1460 and 1570 cm^{-1} observed for the Gd^{3+}-RMPA complex reported by Iben et al [13]. The crystal structure of carp parvalbumin indicates that the Ca^{2+}-binding sites, in the EF and CD domains, have five and six, respectively, oxygen-donating ligands of the CO_2^- variety coordinating Ca^{2+} [15]. Thus, the majority of the ligands coordinated to the Yb^{3+} complexed in the RMPA protein are expected to be of the CO_2^- variety. The observation of the broad sideband at 1500 cm^{-1} which is atributable to CO_2^- modes is consistent with these structural data. There is also observable a sideband at about 2650 cm^{-1} which can be atributable to a C–H stretch based on the Yb^{3+}-methanol VSB spectrum (Fig. 1b).

We have demonstrated that NIR fluorescence vibronic sideband spectroscopy provides vibrational information concerning chelates of Yb^{3+} in total agreement with the UV analogue technique using Gd^{3+}. The model complexes presented here indicate that distinct VSB spectra are obtained and that they may be used as spectroscopic signatures to identify chemical groups in amaino acids which act as ligands to the Yb^{3+} ion. The advantages of this technique are that potentially destructive UV radiation is not used and protein fluorescence which usually requires sophisticated time-resolved techniques is not required. Another benefit is that greater spectral resolution is afforded by the FT Raman spectrometer (4 cm^{-1}) working in the NIR, where the wavelength dispersion is less congested. We have verified with a Photosystem II preparation that 910 nm excitation does not induce

protein fluorescence, which is not the case when the fluorescence of Gd^{3+} complexed to the Ca^{2+} binding site is excited with about 300 nm excitation. Thus, near-infrared vibronic sideband fluorescence spectroscopy using Yb^{3+} to probe the Ca^{2+}-binding site of proteins in general, and of photosynthetic reaction center proteins specifically, should constitute a powerful technique to probe Ca^{2+}-binding sites without complications from protein fluorescence and actinic effects. We are currently improving this technique by fitting our spectrometer with highly efficient cut-off filters to remove stray light from the exciting laser beam to improve signal quality and to allow more efficient pumping of fluorescence by using laser wavelengths closer to the absorption maximum of Yb^{3+} (about 970 nm).

We thank M. Pascal Voluer of Spectra Physics for the loan of the Ti:sapphire laser as well as Drs. Philippe Champeil and Alain Desbois for useful discussions and Eliane Nabedryk for the recording of IR spectra. A.B. was supported by the CNRS.

References

1 Einspahr, H. and Bugg C.E. (1984) in Metal ions in biological systems (Sigel, M., ed.), Vol. 17, pp. 51–107, Dekker, Basel.
2 McPhalen, C.A., Strynadka, N.J.C. and James, M.N.G. (1991) Adv. Protein Chem. 42, pp 77–144.
3 Heizmann, C.W. and Hunziker, W. (1991) Trends Biochem. Sci. 16, 98–103.
4 Rutherford, A.W., Zimmermann, J.-L. and Boussac, A. (1992) in The Photosystems: Structure, Function and Molecular Biology (Barber, J., ed.), Oxygen evolution, pp. 179–229, Elsevier, Amsterdam.
5 Yocum, C.F. (1991) Biochim. Biophys. Acta 1059, 1–15.
6 Debus, R.C. (1992) Biochim. Biophys. Acta, in press.
7 Antanaitis, B.C., Brown, R.D., Chasteen, N.D., Freedman, J.H., Koenig, S.H., Lilienthal, H.R., Peisach, J. and Brewer, C.F. (1987) Biochemistry 26, 7932–7937.
8 Bakou, A., Buser, C., Dandulakis, G., Brudvig, G. and Ghanotakis, D.F. (1992) Biochim. Biophys. Acta 1099, 131–136.
9 Horrocks, W. DeW. (1982) in Advances in Inorganic Biochemistry (Eichorn, G.L. and Marizilli, L.G., eds.), Vol. 4, pp. 201–261, Elsevier, Amsterdam.
10 O'Hara, P.B. (1987) Photochem. Photobiol. 46, 1067–1076.
11 Martin, R.B. and Richardson, F.S. (1979) Q. Rev. Biophys. 12, 181–209.
12 MacGregor, R.B., Jr. (1989) Arch. Biochem. Biophys. 274, 312–316.
13 Iben, I.E.T., Stavola, M., MacGregor, R.B., Zhang, X.Y. and Friedman J.M. (1991) Biophys. J. 59, 1040–1049.
14 Dieke, G.H. (1968) in Spectra and Energy Levels of Rare Earth Ions in Crystals (Crosswhite, H.M. and Crosswhite, H., eds.), Wiley, New York.
15 Kumar, V.D., Lee, L. and Edwards, B.F.P. (1991) FEBS Lett. 283, 311–316.
16 Schrader, B., Hoffmann, A., Simon, A., Podschadlowski, R. and Tischer, M. (1990) J. Mol. Struct. 217, 207–220.
17 Carnall, W.T. (1979) in Handbook on the Physics and Chemistry of the Rare Earths (Gschneider, K.A., Jr. and Eyring, L., eds.), Vol. 3, pp. 171–208, North-Holland, Amsterdam.
18 Barela, T.D. and Sherry, A.D. (1976) Anal. Biochem. 71, 351–357.